Biology Faculty Publications and Presentations

Biology

8-10-2020

Metabolomics Analysis of Annual Killifish (austrofundulus Limnaeus) Embryos During Aerial Dehydration Stress

Daniel Zajic
Portland State University

Jason Podrabsky
Portland State University, podrabsj@pdx.edu

Citation Details

1 **Metabolomics analysis of annual killifish (*Austrofundulus limnaeus*) embryos**
2 **during aerial dehydration stress**
3

4 Daniel E. Zajic[1,2]* and Jason E. Podrabsky[1]
5

6 [1]Department of Biology, Portland State University, P.O. Box 751, Portland, OR 97207
7 [2]Health, Human Performance, and Athletics Department, Linfield University, 900 SE
8 Baker, McMinnville, OR 97128
9

10 ***Corresponding author:**
11 dzajic@linfield.edu
12 Health, Human Performance, and Athletics Department
13 Linfield University
14 900 SE Baker
15 McMinnville, OR 97128
16

17 **Key words:** diapause, antioxidants, 2-hydroxyglutarate, lanthionine, neuroprotection
18

19 **Running title:** Metabolomics of dehydrated killifish embryos
20

21

22 **Author contributions**
23 Conceptualization: D.E.Z., J.E.P.; Methodology: D.E.Z., J.E.P.; Formal analysis: D.E.Z.,
24 J.E.P.; Investigation: D.E.Z., J.E.P.; Data curation: D.E.Z., J.E.P.; Writing - original draft:
25 D.E.Z.; Writing - review & editing: D.E.Z., J.E.P.; Visualization: D.E.Z., J.E.P.;
26 Supervision: J.E.P.; Funding acquisition: J.E.P.

27   **Abstract**

28   The annual killifish, *Austrofundulus limnaeus*, survives in ephemeral ponds in the

29   coastal deserts of Venezuela. Persistence through the dry season is dependent on

30   drought-resistant eggs embedded in the pond sediments during the rainy season. The

31   ability of these embryos to enter drastic metabolic dormancy (diapause) during normal

32   development enables *A. limnaeus* to survive conditions lethal to most other aquatic

33   vertebrates; critical to the survival of the species is the ability of embryos to survive

34   months and perhaps years without access to liquid water. Little is known about the

35   molecular mechanisms that aid in survival of the dry season. This study aims to gain

36   insight into the mechanisms facilitating survival of dehydration stress due to aerial

37   exposure by examining metabolite profiles of dormant and developing embryos. There

38   is strong evidence for unique metabolic profiles based on developmental stage and

39   length of aerial exposure. Actively developing embryos exhibit more robust changes,

40   however, dormant embryos respond in an active manner and significantly alter their

41   metabolic profile. A number of metabolites accumulate in aerial-exposed embryos that

42   may play an important role in survival, including the identification of known antioxidants

43   and neuroprotectants. In addition, a number of unique metabolites not yet discussed in

44   the dehydration literature are identified, such as lanthionine and 2-hydroxyglutarate.

45   Despite high oxygen availability, embryos accumulate the anaerobic end-product

46   lactate. This paper offers an overview of the metabolic changes occurring that may

47   support embryonic survival during dehydration stress due to aerial incubation, which

48   can be functionally tested using genetic and pharmacological approaches.

49

Introduction

50

51   The annual killifish, *Austrofundulus limnaeus*, inhabits temporary pools in the

52   Maracaibo basin of Venezuela. Their habitat is defined by highly unpredictable episodic

53   rain events, which leads to uncertainty in the length of time that a pool will experience

54   inundation. Thus, individual pools may remain dry for months or perhaps years (44, 50,

55   52). During the rainy season, adult *A. limnaeus* deposit their embryos into the often

56   oxygen-limited pool substrate. As the rainy season ends, the adult fish die and embryos

57   must survive severely dehydrating conditions in the mud, often faced with a variety of

58   other stresses such as extremes in temperature and oxygen until the wet season

59   returns and they can complete development (44). As a result, *A. limnaeus* has evolved

60   extremely stress-resistant embryos with the ability to enter a profound state of metabolic

61   depression termed diapause (48, 49). There are three unique stages of diapause (I, II,

62   and III) which an embryo can enter during development (43, 70, 71). The most stress-

63   tolerant stage, diapause II (DII), occurs midway through development and mostly

64   consists of cardiac and neural tissue (48, 51). The developmental ecology of *A.*

65   *limnaeus* embryos has not been characterized in the field. However, embryos of other

66   species of annual killifish are primarily found in DII during the peak of the dry season,

67   and in a variety of post-DII stages during the late dry season (53). Thus, DII is likely

68   primarily responsible for dry season survival in *A. limnaeus,* but tolerance of dehydrating

69   conditions is required during the entire duration of post-DII development.

70   For aquatic organisms, aerial exposure imposes oxygen stress due to an

71   increase in availability compared to most aquatic habitats, but also imposes a severe

72   dehydration stress. A main reason for dehydration injury is attributed to the increased

73   formation of ROS and subsequent oxidative damage due to water stress (14). Free

74   radical formation can lead to lipid peroxidation, denaturation of proteins, and DNA

75   damage which ultimately can affect overall metabolism (18). However, protection

76   against such damage can partially be mitigated by accumulation of antioxidant

77   metabolites, such as glutathione (GSH) (30). Embryos of *A. limnaeus* have a notable

78   tolerance of oxidative stress (65), but the role of antioxidants has not been investigated

79   through the lens of dehydration stress.

80   Embryos of *A. limnaeus* experience unique resistance to dehydration stress that

81   is not seen in other aquatic vertebrates and can survive for over 500 days at 85%

82   relative humidity (RH) (46, 74); however, this ability has received far less attention than

83   other aspects of their biology. When embryos of *A. limnaeus* are aerially incubated, thus

84   exposed to dehydration stress, they initially lose water from the extraembryonic

85   perivitelline space but embryonic compartments remain fully hydrated (46). After a

86   week, water loss approaches zero. Paradoxically, DII embryos respond to aerial

87   dehydration stress by increasing oxygen consumption, while post-diapause II (post-DII)

88   embryos are either unaffected or severely reduce oxygen consumption. The

89   mechanisms that aid survival during dehydration stress and contribute to these

90   metabolic phenotypes are unknown.

91   *Austrofundulus limnaeus* is a promising model organism for developmental

92   physiology and ecology because of their tolerance of a plethora of stresses, annotated

93   genome, and ability to alter developmental trajectories in the lab (43, 47, 54, 64). The

94   current study was performed to expand our knowledge of stress tolerance in *A.*

95   *limnaeus* by exploring the metabolic pathways that may be providing this species with

96   its remarkable abilities to survive extreme dehydration stress. We examine the

97   metabolite profiles of dormant (DII) and actively developing (post-DII) embryos in

98   response to short and long-term aerial dehydration stress (85% RH). We show that

99   actively developing and dormant embryos share metabolic pathways and accumulation

100   of similar metabolites in response to dehydration stress. However, we also see

101   developmentally distinct differences that suggest stage-specific responses. We identify

102   critical roles for amino acid and lipid metabolism, show accumulation of known

103   antioxidant and neuroprotective compounds, and identify novel metabolites produced in

104   response to aerial dehydration stress.

Materials and Methods

Animal husbandry and embryo collection

Adult annual killifish were housed and embryos collected as previously described (45). All work was performed under established protocols that were reviewed and sanctioned by the Portland State University Institutional Animal Care and Use Committee (PSU IACUC protocols #33 and 64). Briefly, adult fish were kept in male-female pairs and spawned semiweekly. Embryos were collected and stored at 25°C with no light in 15 x 100 mm plastic Petri dishes in media that resembles the environmental conditions from which adults were collected in 1995 (10 mmol l^{-1} NaCl, 2.15 mmol l^{-1} $MgCl_2$, 0.8 mmol l^{-1} $CaCl_2$, 0.14 mmol l^{-1} KCl, 1.3 mmol l^{-1} $MgSO_4$) (45, 50). For the first 4 days post-fertilization (dpf), embryo medium contained methylene blue (0.0001%) to prevent fungal infection. Embryos were then treated with two 5 min washes of a 0.01% sodium hypochlorite solution (separated by a 5 min rest in embryo medium) to prevent bacterial and fungal growth, as previously described (45). Following sodium hypochlorite treatment, embryos were transferred to embryo medium containing 10 mg l^{-1} gentamicin sulfate and allowed to develop to DII (32–64 d). To break DII, embryos were subjected to a temperature of 30°C and full spectrum light for 48 h (31). Following this treatment, embryos were sorted into synchronized cohorts of embryos by developmental stage (Wourms' stage [WS]) as described in Podrabsky et al. (43).

Embryonic stages investigated

Experiments were performed on dormant (DII) and actively developing post-DII embryos (43, 70, 71) to identify stage-specific responses to dehydration stress and to capture different levels of dehydration tolerance. DII embryos are metabolically dormant, have halted development, and have a lethal time to 50% mortality (LT_{50}) in aerial incubation (85% relative humidity [RH]) of 325 d (74). DII embryos tend to stay in diapause during aerial exposure. Post-DII embryos are metabolically active, continue developing during aerial exposure when oxygen is not limiting, and have reduced tolerance of dehydrating conditions. When exposed to aerial conditions during early post-DII development (WS 36, 4 days post-diapause II), dehydration tolerance is reduced to an LT_{50} of 84 d. Late

136   post-DII embryos (WS 40–42) have a further reduced ability to survive aerial incubation

137   and exhibit LT_{50} values around 28–29 d (74).

138

139   ***Metabolomics analysis***

140   *Aerial incubation*

141   Embryos were exposed to 85% relative humidity (RH) air at 25°C with no light in a

142   sealed glass desiccator with a porcelain plate shelf (250 mm diameter, 08615B, Fisher

143   Scientific, Hampton, NH, USA). Relative humidity was controlled by using a saturated

144   solution of potassium chloride (750 ml) placed below the shelf and continually mixed

145   with a stir bar to ensure uniform RH within the aerial portion of the chamber (46, 68).

146   Prior to exposure, embryos were treated with sodium hypochlorite (see above) and

147   incubated in embryo medium containing 10 mg l^{-1} gentamicin sulfate for 3 h prior to

148   aerial exposure. Embryos were placed on filter pads containing 2.5 ml embryo medium

149   containing gentamicin. Care was taken to make certain that single embryos were

150   isolated and not touching other embryos. Embryos were then exposed to 85% RH at

151   25°C without light. DII embryos were sampled after 7 and 28 d while post-DII embryos

152   were sampled at 7 (WS 40) and 18 d (WS 42/43). Control embryos (DII and WS 36)

153   were collected at t = 0 by quickly blotting away embryo medium prior to sampling. Six

154   biological replicates (*N* = 6), comprised of 25 embryos each, were flash frozen with

155   liquid N_2 and stored at –80°C until shipped to Metabolon for metabolite profiling. To

156   better visualize the sampling regimen, see **Figure 1.**

157

158   *Metabolon metabolomics analysis*

159   Sample preparation and metabolomics analysis occurred at Metabolon, but is briefly

160   detailed here. Samples were prepared using an automated MicroLab STAR system

161   (Hamilton Company, Reno, NV, USA). Proteins were precipitated with methanol under

162   vigorous shaking for 2 min (Glen Mills GenoGrinder 2000) followed by centrifugation.

163   This method ensured dissociation of small molecules bound to protein, trapped in the

164   precipitated protein matrix, and recovery of chemically diverse metabolites. The

165   resulting extract was divided into four fractions: two for analysis by two separate reverse

166   phase (RP)/UPLC-MS/MS methods with positive ion mode electrospray ionization (ESI),

167 one for analysis by RP/UPLC-MS/MS with negative ion mode ESI, and one for analysis

168 by HILIC/UPLC-MS/MS with negative ion mode ESI. To remove methanol, samples

169 were placed briefly on a TurboVap (Zymark, Hopkinton, MA, USA). The sample extracts

170 were stored overnight under nitrogen before preparation for analysis. Prior to analysis,

171 sample extracts were reconstituted in solvents compatible to each of the four methods

172 described above. Raw data was extracted, peak-identified, and quality control

173 processed using Metabolon's proprietary hardware and software. At the time of

174 analysis, identification of known biochemicals was based on comparison to

175 metabolomic libraries of more than 3300 commercially available purified standard

176 compounds. Several curation procedures were carried out to ensure high quality data

177 and removal of those data representing system artifacts, mis-assignments, and

178 background noise. The present dataset comprises a total of 673 compounds of known

179 identity (metabolites). Data for each metabolite is presented relative to control samples

180 (t = 0) and expressed as non-normalized, protein-normalized (Bradford assay), and

181 DNA-normalized (Table 1). Due to the changing amount of water in the samples over

182 the course of aerial incubation, and continued development in post-DII embryos, we

183 have chosen to use the DNA-normalized data to most accurately reflect the relative

184 amounts of metabolites per cell. Bradford protein concentration increases in a linear

185 manner during dehydration while at the same time embryo mass decreases in a similar

186 manner (Supplemental Fig S1; for all supplementary material see

187 https://doi.org/10.6084/m9.figshare.12502085). We interpret this pattern as an artifact of

188 water loss (especially in the DII embryos which are dormant) and so normalization per

189 protein would exaggerate fold changes.

190

191 ***Statistical analysis***

192 Graphical and statistical analyses were performed using Prism 8.0 software (GraphPad,

193 La Jolla, CA, USA) or through Metabolon's user interface. Statistical significance was

194 set to $P < 0.05$ for all comparisons. For metabolomics data analysis, missing values due

195 to being under the limit of detection of the instruments were imputed with the minimum

196 value on a per metabolite basis. For each metabolite, raw counts were scaled to set the

197 median across all samples for that metabolite to 1 and the data log transformed.

198   Following normalization to Bradford protein or DNA concentration, Welch's two-sample

199   t-test was used to identify metabolites that differed significantly between treatments,

200   with a threshold for statistical significance set to $P < 0.05$. Additionally, an estimate of

201   the false discovery rate (q-value) was calculated to take into account the multiple

202   comparisons that normally occur in metabolomic-based studies. A low q-value ($q <$

203   0.10) is an indication of high confidence in a result. Thus, only metabolites with $P < 0.05$

204   and $q < 0.10$ are considered significant in this study. Pathway enrichment analysis was

205   performed using MetaboLync (Metabolon Inc.) with all metabolites and their pre-

206   assigned pathways as background and reference pathways, respectively. Enriched

207   pathways were calculated based on the following formula, where significance was

208   defined as $P < 0.05$:

209   Enrichment value = (k/m)/((n-k)/(N-m))

210   Where: k, total number of significant metabolites in pathway; m, total number of

211   detected metabolites in pathway; n, total number of significant metabolites; N, total

212   number of detected metabolites in the study. A pathway enrichment value greater than

213   one indicates that the pathway contains more significantly changed compounds relative

214   to the study overall. Fisher's exact test ($P < 0.05$) was used to determine if pathway

215   enrichment was significant.

216

Results and Discussion

218

219   This is the first metabolomics study to explore the profound ability of *A. limnaeus*

220   embryos to survive prolonged aerial dehydration stress. The metabolic profiles of DII

221   and post-DII embryos vary greatly, but due to continued development of post-DII

222   embryos during dehydration stress, we cannot confirm if the metabolites accumulated in

223   post-DII embryos are dehydration-specific or developmentally regulated. It is also

224   important to note that the levels of metabolites reported in this paper are from whole

225   embryos. The location of the metabolites, whether they be in the developing embryo,

226   yolk, or perivitelline fluid, is not known. Recognizing the limitations of this study, we

227   introduce new insights into survival of embryos of *A. limnaeus* to aerial dehydration

228   stress by focusing on pathways and metabolites that change in a similar manner in both

229   dormant (DII) and actively developing (post-DII) embryos. Below we outline metabolic

230   pathways and metabolites of interest that may be supporting survival of *A. limnaeus*

231   during dehydration stress induced by aerial exposure.

232

233   ***Metabolomics profiles overview***

234   We measured a total of 673 metabolites of known identity (Supplemental Table S1). A

235   summary of metabolites that achieved statistical significance ($P < 0.05$) using various

236   methods of normalization are presented in Table 1. We provide lists of the top

237   significantly downregulated and upregulated metabolites in response to short-term or

238   long-term aerial incubation in DII and post-DII embryos (Supplemental Tables S2–S9).

239   Although the method of normalization is important, it does not affect the statistical

240   significance of the vast majority of compounds that experience large fold-changes

241   during aerial dehydration stress (see boldface metabolites in Supplemental Tables S2–

242   S9). Here we focus on data normalized to total DNA content to take into account the

243   developmental changes that occur in post-DII embryos. Overall metabolite abundance

244   was found to generally increase following aerial exposures, with the exception of short-

245   term incubation of post-DII embryos (Table 1). These changes in metabolites, especially

246   in DII embryos, indicate a large-scale active response to aerial dehydration stress. The

247   increase in some metabolites is consistent with the observed rise in oxygen

248   consumption seen in DII embryos when exposed to aerial conditions (74).

249

250   **Superpathways**

251   Metabolites were categorized as belonging to 1 of 8 superpathways (Fig 2). Of the

252   metabolites measured, 70% belonged to lipid (N = 306) and amino acid (N = 164)

253   metabolism. The remaining 30% belonged to nucleotide (N = 70), carbohydrate (N =

254   42), cofactors and vitamins (N = 30), xenobiotics (N = 30), peptide (N = 20), and energy

255   metabolism (N = 11). Within each superpathway, metabolites were clustered based on

256   81 subpathways (Fig 2).

257

258   **Enriched subpathways**

259   *Diapause II.*

260   Seven subpathways were enriched in DII embryos following short-term aerial

261   dehydration stress and 4 were enriched during long-term exposures (Table 2). The most

262   enriched pathways were associated with fatty acid and amino acid metabolism.

263   Additionally, nicotinate and nicotinamide metabolism was enriched. The amino acid

264   subpathways enriched are shared between long-term and short-term exposures.

265

266   *Post-DII embryos.*

267   In general, there was more variation in pathway enrichment in post-DII embryos

268   compared to DII embryos (Table 2). There were 10 enriched subpathways in response

269   to short-term (N = 5) and long-term (N = 5) aerial incubation. Most enriched pathways

270   belonged to lipid and amino acid metabolism. There were three pathways that were

271   consistently enriched during short and long-term exposures: phosphatidylcholine (PC),

272   gamma-glutamyl amino acid, and monoacylglycerol metabolism.

273

274   **Shared metabolites (long-term dehydration)**

275   Due to continued development of post-DII embryos during dehydration exposure, we

276   chose to focus on metabolites that showed shared responses (upregulation or

277   downregulation) in DII and post-DII embryos in response to aerial dehydration stress.

10

278 Since DII embryos remained in diapause, we can more easily attribute metabolic

279 change as primarily a direct response to dehydration stress and not an effect of active

280 development. DII embryos have a suppressed metabolism, thus changes in metabolic

281 profiles may not be apparent after short-term incubation. We therefore chose to focus

282 on metabolites shared following long-term exposures.

283   When compared to controls, there were a total of 71 shared metabolites that

284 significantly increased during long-term exposures (Fig 3); whereas there were only 18

285 metabolites that decreased (Fig 3). Of the metabolites that increased, 48 belonged to

286 lipid (N = 24) and amino acid (N = 24) metabolism. The remainder belonged to

287 carbohydrate (N = 8), nucleotide (N = 7), xenobiotics (N = 6), cofactors and vitamins (N

288 = 1), and peptide metabolism (N = 1). Of the metabolites that decreased, a majority

289 belonged to monoacylglycerol metabolism (N = 11). The remaining downregulated

290 metabolites belonged to nucleotide (N = 2), cofactors and vitamins (N = 2), amino acid

291 (N = 1), carbohydrate (N = 1), and xenobiotics (N = 1) metabolism.

292   Many of these metabolites are in pathways found to be enriched in response to

293 short or long-term aerial incubation (Table 2). In addition to those enriched pathways,

294 there are several metabolites that belong to shared pathways that will be explored

295 further below.

296

297 **_Pathways of interest_**

298 _Amino acids and dipeptides_

299 _Methionine, Cysteine, and Gamma-Glutamyl Amino Acids_. There are indications of

300 altered transsulfuration activity and antioxidant demand and utilization in embryos

301 exposed to aerial dehydration stress (Fig 4). Transsulfuration is a highly conserved

302 pathway involved in metabolizing sulfur-containing amino acids such as methionine and

303 cysteine. Methionine, via the transsulfuration pathway, can be converted to cysteine and

304 several other compounds that play roles in redox balance and antioxidant defense (e.g.,

305 glutathione, taurine, etc.). Notably, an increase in cystathionine is observed in both DII

306 and post-DII embryos (Figs 3,4).

307   The metabolite with the largest fold-change in this study is lanthionine (Fig 3;

308 greater than 800-fold increase in post-DII embryos). Lanthionine is formed when

11

309 cysteine is metabolized in lieu of homocysteine or cystathionine by the transsulfuration

310 pathway enzymes cystathionine β-synthase (CBS) and cystathionine γ-lyase (CSE) (Fig

311 4). A common product of lanthionine biosynthesis is hydrogen sulfide (H_2S), which has

312 been recognized as an important biological signaling molecule (11, 38). H_2S has been

313 shown to protect heart mitochondrial function during ischemic events and induce a state

314 of suspended animation associated with a lower metabolism and body temperature in

315 mice (4, 11). In addition, lanthionine can also be further metabolized in mammalian

316 brain tissue to form the cyclic thioether, lanthionine ketimine, which is known to be

317 associated with high affinity (58 nmol) to neuronal membranes (13) and has been

318 demonstrated to have neuroprotective, neurotrophic and anti-inflammatory activities in

319 mice during cerebral ischemia (19, 35). Embryos of *A. limnaeus* may experience

320 dehydrating conditions for months and perhaps years before water returns (44, 52) and

321 very likely depend on suppression of metabolism and induction of cellular protective

322 mechanisms for survival (74). Thus, it is possible that lanthionine accumulation may

323 support long-term survival of dehydration stress through suppression of metabolism

324 mediated by H_2S production, and through the cytoprotective actions of lanthionine

325 ketimine in cardiac and neural tissues.

326   The large observed increase in lanthionine suggests a potential role as a

327 compatible osmolyte. However, in the relatively few studies that exist, elevated

328 lanthionine (0.3–2 μmol l^{-1}) appears to have generally negative effects on fish embryo

329 physiology and development, though some of these effects were counteracted with

330 addition of glutathione (42). Lanthionine may also interfere with angiogenic signaling,

331 increasing intracellular calcium, and impairing H_2S production (42, 63). Thus, the ability

332 of *A. limnaeus* embryos to tolerate such large increases in lanthionine without apparent

333 negative effects is interesting. Although we do not know the concentrations of

334 lanthionine in embryos of *A. limnaeus*, an 800-fold change from even the picomolar

335 level would reach biologically relevant concentrations (42). The biology of lanthionine,

336 and its association with survival of long-term dehydration stress warrants further

337 investigation.

338   Both the oxidized and reduced forms of glutathione (GSSG and GSH,

339 respectively) were found to be accumulated in post-DII embryos, whereas only GSSG

340   was increased in abundance in DII embryos. Cells use glutathione to scavenge reactive

341   oxygen species (ROS) in order to reduce oxidative damage. A previous study showed a

342   significant increase in total glutathione content in *A. limnaeus* embryos during post-DII

343   development (65). However, close to 100% of the glutathione measured was in its

344   reduced form, thus the increases in GSSG observed in this study appear to be the

345   result of aerial incubation. In their natural habitat, *A. limnaeus* embryos are exposed to a

346   variety of conditions (e.g. hypoxia, high temperatures) as they endure the dehydrating

347   conditions of the dry season, which could lead to increases in ROS production. A rise in

348   GSSG is usually indicative of some form of oxidative stress. One explanation for the

349   observed rise in GSSG in DII embryos may be due to increased oxidative stress as a

350   consequence of increased oxygen availability and increased oxygen consumption

351   observed in response to aerial dehydration stress (74). Another possibility is that GSSG

352   is assisting in reducing protein synthesis during dehydration, as GSSG is a known

353   potent inhibitor of protein synthesis (12).

354   Post-DII embryos also display significant decreases in 5-oxoproline, an

355   intermediate of gamma-glutamyl amino acid metabolism, which could be reflective of

356   changes in glutathione recycling. Fourteen gamma-glutamyl metabolites decreased in

357   aerially incubated post-DII embryos and not surprisingly this pathway is enriched in

358   post-DII embryos (Table 2; Fig 5). The function of the gamma-glutamyl pathway is

359   somewhat controversial. The original theory suggested the main function was amino

360   acid transport into the cell via their conversion to gamma-glutamyl amino acids, a

361   glutathione-dependent process (39). The release of amino acids from gamma-glutamyl

362   amino acids by gamma-glutamyl cyclotransferase generates 5-oxoproline as an

363   intermediate (Fig 4). However, recent findings suggest a role for the gamma-glutamyl

364   cycle as a regulator of redox metabolism of free radicals and xenobiotics (22). A recent

365   review by Bachhawat and Yadav proposes a "glutathione cycle" to replace the

366   established gamma-glutamyl cycle (2). The discrepancies in these cycles is beyond the

367   scope of this article, but there is a clear role for both glutathione and gamma-glutamyl

368   metabolism in *A. limnaeus* embryos worth further exploration.

369

13

370   *Tryptophan Metabolism.* There were 2 metabolites that increased in the pathway for

371   metabolism of tryptophan: C-glycosyltryptophan and picolinate. Of note is picolinate,

372   which exhibited a 65-fold change in DII embryos (Fig 3; Supplemental Tables S2–5).

373   The large increase observed in metabolically suppressed embryos suggests an

374   important role for picolinate, a small molecule with known neuroprotective,

375   immunological, and anti-proliferative effects (5, 17) in survival of aerial dehydration

376   stress.

377

378   *Creatine Metabolism.* DII and post-DII embryos exhibited different creatine metabolite

379   profiles (Fig 6). Creatine phosphate (PCr) serves as a diffusible high-energy phosphate

380   reserve in vertebrate cells. The accumulation of PCr in DII embryos indicates a positive

381   energy balance and is consistent with previous reports of high ATP/ADP ratios during

382   diapause (48). The decline in PCr and subsequent rise in creatine in post-DII embryos

383   suggests that ATP demand is outpacing ATP production. This may suggest that aerial

384   exposure is a metabolic stress for post-DII embryos and not for DII embryos. In addition

385   to its role in buffering cellular ATP levels, creatine and PCr have been shown to exhibit

386   a number of cytoprotective effects associated with membranes including: stabilization,

387   alteration of phase transition temperature, and reduction of leak (62). Additionally, PCr

388   can have protective effects against ischemic injury (26, 56). Thus, the accumulation of

389   PCr in DII embryos may offer protective effects that contribute to their much higher

390   tolerance of aerial dehydration stress compared to post-DII embryos.

391

392   *Glutamate Metabolism.* Gamma-aminobutyrate (GABA) is accumulated in both DII (1.6-

393   fold) and post-DII embryos (20-fold) during long-term exposures (Fig 3; Supplemental

394   Table S5). GABA is known to accumulate during anoxia in embryos of *A. limnaeus* and

395   blocking GABA production reduces anoxic survival (51, 75). When GABA is measured

396   spectrophotometrically, it is often undetectable during normal *A. limnaeus* development

397   (75). Thus, the amount of GABA accumulating during dehydration stress probably

398   represents micromolar quantities, and not millimolar levels as seen during anoxia (75).

399   GABA is known to have neuroprotective roles in organisms (21, 36), and is also

400   important in reducing ROS production and protecting against oxidative stress in yeast

401 (7). Although the levels are likely lower than during anoxia, GABA may still have an

402 important role as a neuroprotective and antioxidant agent during exposures to

403 dehydration.

404

405 *Carbohydrate*

406 *Glycolysis, Gluconeogenesis, and Pyruvate Metabolism and the Pentose Phosphate*

407 *Pathways*. There were 4 metabolites from these pathways that increased in both DII

408 and post-DII embryos: Glucose-6-phosphate, pyruvate, lactate, and sedoheptulose-7-

409 phosphate (Figs 3,7). There were also two stage-specific metabolites that accumulated:

410 glycerate in DII, and phosphoenolpyruvate (PEP) in post-DII embryos (Fig 7;

411 Supplemental Tables S2–4). We previously hypothesized that aerial dehydration stress

412 would limit gas exchange with the environment in concert with the observed decrease in

413 evaporative water loss (46) and lead to self-imposed hypoxia or anoxia. The large

414 increase in GABA and lactate in post-DII embryos supports this hypothesis. Further, the

415 relatively small fold-change in lactate and GABA for DII embryos is consistent with their

416 increase in oxygen consumption in response to aerial dehydration stress (74). Thus,

417 these metabolomics data are consistent with hypoxic metabolism in post-DII but not DII

418 embryos during long-term dehydration stress. Interestingly, the increase in lactate

419 resembles that of the Warburg effect, which is commonly observed in many cancer

420 cells, where enhanced glycolysis and lactate fermentation occur even in the presence of

421 sufficient oxygen. Relying partially on anaerobic mechanisms may offset the reliance on

422 aerobic metabolism which can ultimately lead to increases in ROS. Additionally, lactate

423 in appropriate amounts has been shown to help regulate gene expression through

424 inhibition of histone deacetylase activity and post-translational modifications of histones,

425 act in a neuroprotective role by preventing excitotoxic cell death, and promote oxidative

426 stress resistance (3, 27, 61, 77). Thus, aerobic accumulation of lactate may help fuel a

427 response to dehydration stress through a variety of mechanisms outside of its role in the

428 maintenance of cytoplasmic redox balance.

429 The accumulation of glucose-6-phosphate and sedoheptulose-7-phosphate

430 (S7P) is consistent with activation of the pentose phosphate pathway (PPP; Fig 7) (41).

431 Shunting of carbon into the PPP results in the production of NADPH used to support

432   anabolic processes, and also critical for the regeneration of reduced glutathione (33,

433   41). Accumulation of S7P, but not glyceraldehyde-3-phosphate (G3P) suggests that the

434   oxidative portion of the PPP is used to produce NADPH, but not all of the carbon is

435   shuttled back into glycolysis and instead is allowed to accumulate as S7P. In addition,

436   the accumulation of several ribose metabolism intermediates (Fig 3) is also consistent

437   with increased flux through the PPP. This hypothesis provides a mechanism to support

438   antioxidant capacity (see above discussion of glutathione) while allowing limited

439   immediate carbon flow through glycolysis in the form of G3P, and accumulating a

440   source of carbon (S7P) that could be readily utilized by glycolysis at a later time. These

441   data suggest a critical role for the PPP in supporting aerial dehydration stress in *A.*

442   *limnaeus* embryos.

443

444   *Lipids*

445   *Fatty Acid, Dicarboxylate*. Seven metabolites increased following long-term dehydration:

446   Glutarate (C5-DC), 3-methylglutarate/2-methylglutarate, 2-hydroxyglutarate, adipate

447   (C6-DC), 3-hydroxyadipate, maleate, and sebacate (C10-DC) (Fig 3). Of interest is the

448   accumulation of 2-hydroxyglutarate (2-HG), a molecule known to be produced during

449   hypoxia and a known oncometabolite (23, 37, 66) that can inhibit alpha-ketoglutarate-

450   dependent enzymes involved in many biological processes (73). TET enzymes (DNA

451   demethylases) and histone demethylases are inhibited by 2-HG which can lead to

452   changes in the epigenetic landscape of cells and large-scale changes in gene

453   expression (10, 24, 73). There are several routes for production of 2-HG, including

454   through 'promiscuous' reduction of alpha-ketoglutarate by lactate dehydrogenase and

455   malate dehydrogenase (23, 24). Further, 2-HG has been shown to inhibit ATP synthase

456   activity and extend lifespan of *Caenorhabditis elegans* (15) suggesting this molecule

457   could have a number of beneficial effects on *A. limnaeus* embryos during dehydration

458   stress due to aerial incubation.

459

460   *Fatty Acid, Acyl carnitine*. Several acyl carnitine metabolites ($N = 5$) were upregulated:

461   arachidoylcarnitine (C20), arachidonoylcarnitine (C20:4), docosapentaenoylcarnitine

462   (C22:5n6), stearoylcarnitine (C18), palmitoleoylcarnitine (C16:1) (Fig 3). Acyl carnitines

16

463   play an essential role in regulating the balance of intracellular sugar and lipid

464   metabolism (28) primarily as carriers for long-chain fatty acids into mitochondria to

465   support β-oxidation (28, 60). Accumulation of these metabolites may suggest reduced

466   mitochondrial fatty acid metabolism during aerial incubation.

467

468   *Phospholipid*s. The only metabolite in the phospholipid subpathway to be accumulated

469   in both DII and post-DII embryos was cytidine 5'-diphosphocholine (Fig 3). Cytidine 5'-

470   diphosphocholine is an intermediate product of phosphatidylcholine synthesis. The

471   compound has been used extensively in clinical settings to treat patients with

472   neurological disorders, including cerebral ischemia. The main protective role of cytidine

473   5'-diphosphocholine is through membrane stabilization (78). Further research has

474   shown cytidine 5'-diphosphocholine protects rat livers from ischemia and reperfusion

475   injury, thus preserving mitochondrial function and reducing oxidative stress (76).

476   Stabilization of cell membranes and reduction of free radical generation may be

477   beneficial to survival of *A. limnaeus* embryos during aerial dehydration stress.

478

479   *Bile Acid Metabolism.* Both taurolithocholate and taurochenodeoxycholate accumulate

480   during long-term exposures (Fig 3). Taurolithocholate accumulates to higher levels in

481   DII embryos (almost 10-fold), while taurochenodeoxycholate exhibits an over 100-fold

482   increase in post-DII embryos. In general, bile acids are toxic due to their ability to act as

483   detergents, but the tauro-derivatives of bile acids tend to be less toxic (55). It is

484   interesting that DII embryos accumulate bile acids despite the absence of liver tissue. In

485   addition to their role in digestion, bile acids can act as signaling molecules via a variety

486   of pathways, including the regulation of a number of nuclear receptors (20). It is

487   possible that these potentially toxic compounds are produced to activate signaling

488   pathways that help support survival. This possibility is intriguing and warrants further

489   investigation.

490

491   *Cofactors and Vitamins*

492   *Nicotinate and Nicotinamide metabolism.* Metabolites linked to *de novo* and salvage

493   (nicotinamide, nicotinamide riboside, nicotinamide ribonucleotide, and nicotinate)

494   pathways of NAD+ synthesis were found to be significantly altered in response to aerial

495   exposure in both DII and post-DII embryos (Fig 8). One difference between DII and

496   post-DII embryos was the significant accumulation of nicotinamide adenine dinucleotide

497   (NAD+) in DII embryos (Fig 8; 17-fold increase). NAD+ is a coenzyme that plays a vital

498   role in redox reactions associated with glycolysis, the TCA cycle, and oxidative

499   phosphorylation. Increasing NAD+ levels in mammals has been linked to improved

500   mitochondrial function under stress (6, 8). Enhancing NAD+ availability in *C. elegans*

501   has been shown to increase lifespan and protect against ROS (34). Conversely,

502   reduction in NAD+ levels is an indication of senescence, as seen in various animal cell

503   lines (16, 34). There is an initial rise in quinolinate in DII embryos followed by a

504   decrease after long-term exposure. It is likely that the decrease in quinolinate

505   contributed to the increase in NAD+ via *de novo* synthesis (Fig 8). The overall rise in

506   NAD+ in DII embryos and maintained levels in post-DII embryos following long-term

507   dehydration stress suggest changes in both demand and synthesis. The accumulation

508   of NAD+ in DII suggests an available pool of NAD+ to contribute to metabolism, while

509   the static levels of NAD+ in post-DII embryos suggests supply and demand are in

510   synergy. The rise in the associated metabolites in the pathway provide a molecular

511   supply for further synthesis of NAD+ via the salvage pathway.

512

513   *Xenobiotics*

514   Xenobiotics refer to compounds not expected to be present within an organism. There

515   were several metabolites that accumulated which are traditionally thought to be

516   produced by animal microbiomes including: 3 tyrosine metabolites (phenol sulfate, 4-

517   hydroxyphenylpyruvate, and 3-methoxytyrosine) and 3 benzoate metabolites (hippurate,

518   guaiacol sulfate, p-cresol sulfate). Both DII and post-DII embryos exhibited an over 50-

519   fold increase in phenol-sulfate following long-term exposures and hippurate increased

520   over 100-fold in DII embryos (Fig 3). Of these metabolites, hippurate and p-cresol

521   sulfate are known markers for microbiome diversity (40). Hippurate, along with other

522   benzoates, has been shown to inhibit the growth of tumors in mouse cell lines (58). The

523   accumulation of these metabolites in *A. limnaeus* is interesting and may suggest a

524   maternally packaged microbiome in these embryos. While it is possible that these

18

525 compounds accumulate due to microbial growth on the surface of the embryos, this is

526 unlikely given the use of antibiotics in the medium, the detection of these metabolites at

527 t = 0, and the lack of other more general microbially-derived compounds that would be

528 expected to accumulate. Interestingly, there is evidence of specific enzymes in the yolk

529 sacs of chicken and tortoise embryos that are capable of producing metabolites that

530 otherwise only exist in microorganisms and plants (9). For example, chicken embryos

531 synthesize lanthionine via enzymes exclusively found in yolk sac endodermal cells.

532 These enzymes disappear upon hatching, which may help explain the lack of

533 lanthionine references in the literature. Alternatively, it is possible that these metabolites

534 are produced by a yolk sac specific microbiome that aids in survival of dehydration

535 stress. Further research needs to be done to elucidate the location, origin, and role of

536 these metabolites in *A. limnaeus* embryos.

537

538 *Conclusions and Future Directions*

539 The goal of this metabolic profiling study was to gain insight into the biochemical

540 pathways facilitating survival of aerial dehydration stress in *A. limnaeus* embryos. There

541 is evidence of a robust metabolic response to aerial dehydration stress even in

542 metabolically dormant embryos. Evidence exists for a progressive imposition of hypoxia

543 in long-term responses to aerial dehydration stress in post-DII embryos but not during

544 diapause. However, further studies need to be done to delineate whether the responses

545 seen in the post-DII embryos are developmental differences or dehydration-specific

546 responses. In general, amino acid and lipid metabolism appear to play central roles in

547 metabolic adjustments during aerial dehydration stress, and it is clear that embryos are

548 not solely relying on carbohydrate reserves to fuel metabolism. Increased capacity for

549 detoxification of ROS and maintenance of redox balance appear to be of major

550 importance to supporting development and surviving under aerial dehydration stress. It

551 is also interesting that several accumulated metabolites have previously been identified

552 as neuroprotectants. This work offers a first glimpse into the metabolic programs that

553 may support survival of long-term aerial dehydration stress in embryos of *A. limnaeus*

554 that can be functionally tested using genetic and pharmacological approaches.

555

556   *Perspectives*

557   Embryos of *A. limnaeus* likely spend many months, the preponderance of their life span,

558   aerially incubated in the wild. During aerial exposure, there are a number of metabolites

559   accumulated that are usually associated with waste or have the potential to be toxic

560   (e.g., bile acids, hippurate, lanthionine). Many of these compounds contain nitrogen or

561   other typical waste products of metabolism that are excreted in the urine and feces.

562   When exposed to aerial conditions, embryos of annual killifish must presumably rely on

563   detoxification or compartmentalization of waste product metabolites to ensure the

564   developing embryo remains unharmed. One possible compartment for storage of waste

565   products is the yolk. It is possible that metabolites are being shuttled into the yolk to

566   protect the developing tissues, as seen with sequestration of ammonia in the yolk sac of

567   rainbow trout (59). In amniotic eggs, the eggs of terrestrial vertebrates, waste is

568   transported from the developing embryo into extraembryonic compartments, notably the

569   amnionic, and the allantoic fluid (1, 32, 67). In the anamniotic eggs of fish, waste

570   products such as ammonia or bile acids can be relatively easily lost due to diffusion into

571   the perivitelline fluid during early development, and excretion during late development

572   as the chorion is not a substantial barrier for diffusion of relatively small metabolites

573   (72). However, in *A. limnaeus* the perivitelline fluid is quickly lost during aerial

574   exposures and can no longer function as a mechanism for diffusive loss of metabolic

575   waste products. Indeed, the embryos of annual killifish embryos exposed to aerial

576   incubation have several unique features that approximate the functions of the shell and

577   extraembryonic components of the amniotic eggs of terrestrial species. First, the egg

578   envelope of annual killifish lacks pores, is substantially thicker than in most species of

579   fish, and may serve a physical role in protection of embryos encased in dry mud (57).

580   Second, the enveloping cell layer of annual killifish embryos does not contribute to the

581   skin of the developing embryos as it does in most fishes, instead it forms a syncytial

582   membrane that surrounds the embryo and is shed upon hatching (69). This membrane

583   constitutes the major permeability barrier between the embryo and its environment and

584   has a unique structure with few embedded proteins (25) and an extremely low

585   permeability to water and salts (29). The enveloping layer in annual killifishes effectively

586   creates an extra-embryonic membrane-bound compartment that surrounds and protects

20

587 the embryo in a manner similar to an amniotic chamber in terrestrial eggs. Thus, it is

588 possible that a number of the compounds that are typically excreted as waste may be

589 stored in either the yolk sac, or in extraembryonic fluid bound by the enveloping cell

590 layer. In fact, many of the accumulated compounds identified in this study are known

591 components of amniotic and allantoic fluid in other species (1, 32, 67) and may suggest

592 a unique extraembryonic compartment in annual killifish embryos. Further exploration

593 into the localization of these metabolites will help elucidate their possible function during

594 survival of dehydration stress due to aerial incubation.

595

596

603

604 **Disclosures**

605 The authors declare no competing interests.

606

607

21

References

610   1.   **Aktuğ T, Uçan B, Olguner M, Akgür F, Özer E, Calişkan S, and Önvural B**.
Amnio-allantoic fluid exchange for the prevention of intestinal damage in gastroschisis
III: determination of the waste products removed by exchange. *European journal of
pediatric surgery* 8: 326-328, 1998.

2.   **Bachhawat AK, and Yadav S**. The glutathione cycle: Glutathione metabolism
beyond the γ-glutamyl cycle. *IUBMB life* 70: 585-592, 2018.

3.   **Berthet C, Lei H, Thevenet J, Gruetter R, Magistretti PJ, and Hirt L**.
Neuroprotective role of lactate after cerebral ischemia. *Journal of Cerebral Blood Flow &
Metabolism* 29: 1780-1789, 2009.

4.   **Blackstone E, Morrison M, and Roth MB**. H_2S induces a suspended animation-
like state in mice. *Science* 308: 518, 2005.

5.   **Bosco MC, Rapisarda A, Massazza S, Melillo G, Young H, and Varesio L**.
The tryptophan catabolite picolinic acid selectively induces the chemokines macrophage
inflammatory protein-1α and-1β in macrophages. *The Journal of Immunology* 164:
3283-3291, 2000.

6.   **Canto C, Menzies KJ, and Auwerx J**. NAD+ metabolism and the control of
energy homeostasis: a balancing act between mitochondria and the nucleus. *Cell
metabolism* 22: 31-53, 2015.

7.   **Cao J, Barbosa JM, Singh NK, and Locy RD**. GABA shunt mediates
thermotolerance in *Saccharomyces cerevisiae* by reducing reactive oxygen production.
Yeast 30: 129-144, 2013.

8.   **Cerutti R, Pirinen E, Lamperti C, Marchet S, Sauve AA, Li W, Leoni V, Schon
EA, Dantzer F, and Auwerx J**. NAD+-dependent activation of Sirt1 corrects the
phenotype in a mouse model of mitochondrial disease. *Cell metabolism* 19: 1042-1049,
2014.

9.   **Chapeville F, and Fromageot P**. "Vestigial" enzymes during embryonic
development. *Advances in Enzyme Regulation* 5: 155-158, 1967.

10.   **Charitou P, Rodriguez-Colman M, Gerrits J, van Triest M, Koerkamp MG,
Hornsveld M, Holstege F, Verhoeven-Duif NM, and Burgering BM**. FOXOs support
the metabolic requirements of normal and tumor cells by promoting IDH1 expression.
EMBO Reports 16: 456-466, 2015.

11.   **Elrod JW, Calvert JW, Morrison J, Doeller JE, Kraus DW, Tao L, Jiao X,
Scalia R, Kiss L, and Szabo C**. Hydrogen sulfide attenuates myocardial ischemia-
reperfusion injury by preservation of mitochondrial function. *Proceedings of the National
Academy of Sciences of the United States of America* 104: 15560-15565, 2007.

12.   **Ernst V, Levin DH, and London IM**. Inhibition of protein synthesis initiation by
oxidized glutathione: activation of a protein kinase that phosphorylates the α subunit of
eukaryotic initiation factor 2. *Proceedings of the National Academy of Sciences of the
United States of America* 75: 4110-4114, 1978.

13.   **Fontana M, Ricci G, Solinas S, Antonucci A, Serao I, Dupre S, and Cavallini
D**. [^{35}S] Lanthionine ketimine binding to bovine brain membranes. *Biochemical and
biophysical research communications* 171: 480-486, 1990.

652 14. **França M, Panek A, and Eleutherio E**. Oxidative stress and its effects during
653 dehydration. *Comparative Biochemistry and Physiology Part A: Molecular & Integrative*
654 *Physiology* 146: 621-631, 2007.
655 15. **Fu X, Chin RM, Vergnes L, Hwang H, Deng G, Xing Y, Pai MY, Li S, Ta L, and**
656 **Fazlollahi F**. 2-Hydroxyglutarate inhibits ATP synthase and mTOR signaling. *Cell*
657 *Metabolism* 22: 508-515, 2015.
658 16. **Gomes AP, Price NL, Ling AJ, Moslehi JJ, Montgomery MK, Rajman L,**
659 **White JP, Teodoro JS, Wrann CD, and Hubbard BP**. Declining NAD+ induces a
660 pseudohypoxic state disrupting nuclear-mitochondrial communication during aging. *Cell*
661 155: 1624-1638, 2013.
662 17. **Grant R, Coggan S, and Smythe G**. The physiological action of picolinic acid in
663 the human brain. *International Journal of Tryptophan Research* 2: IJTR-S2469, 2009.
664 18. **Hansen JM, Go Y-M, and Jones DP**. Nuclear and mitochondrial
665 compartmentation of oxidative stress and redox signaling. *Annual Review of*
666 *Pharmacology and Toxicology* 46: 215-234, 2006.
667 19. **Hensley K, Venkova K, and Christov A**. Emerging biological importance of
668 central nervous system lanthionines. *Molecules* 15: 5581-5594, 2010.
669 20. **Hylemon PB, Zhou H, Pandak WM, Ren S, Gil G, and Dent P**. Bile acids as
670 regulatory molecules. *Journal of Lipid Research* 50: 1509-1520, 2009.
671 21. **Hylland P, and Nilsson GE**. Extracellular levels of amino acid neurotransmitters
672 during anoxia and forced energy deficiency in crucian carp brain. *Brain research* 823:
673 49-58, 1999.
674 22. **Inoue M**. Glutathionists in the battlefield of gamma-glutamyl cycle. *Archives of*
675 *biochemistry and biophysics* 595: 61-63, 2016.
676 23. **Intlekofer AM, Dematteo RG, Venneti S, Finley LW, Lu C, Judkins AR,**
677 **Rustenburg AS, Grinaway PB, Chodera JD, and Cross JR**. Hypoxia induces
678 production of L-2-hydroxyglutarate. *Cell metabolism* 22: 304-311, 2015.
679 24. **Intlekofer AM, Wang B, Liu H, Shah H, Carmona-Fontaine C, Rustenburg**
680 **AS, Salah S, Gunner MR, Chodera JD, and Cross JR**. L-2-Hydroxyglutarate
681 production arises from noncanonical enzyme function at acidic pH. *Nature chemical*
682 *biology* 13: 494, 2017.
683 25. **Jorgenson N-C, and Schmalbruch H**. The eggs of the freshwater fish *Epiplatys*
684 *dageti* have tight plasma membranes without intramembranous particles. *Cell and*
685 *Tissue Research* 235: 643-646, 1984.
686 26. **Landoni G, Zangrillo A, Lomivorotov VV, Likhvantsev V, Ma J, De Simone F,**
687 **and Fominskiy E**. Cardiac protection with phosphocreatine: a meta-analysis.
688 *Interactive Cardiovascular and Thoracic Surgery* 23: 637-646, 2016.
689 27. **Latham T, Mackay L, Sproul D, Karim M, Culley J, Harrison DJ, Hayward L,**
690 **Langridge-Smith P, Gilbert N, and Ramsahoye BH**. Lactate, a product of glycolytic
691 metabolism, inhibits histone deacetylase activity and promotes changes in gene
692 expression. *Nucleic Acids Research* 40: 4794-4803, 2012.
693 28. **Li S, Gao D, and Jiang Y**. Function, detection and alteration of acylcarnitine
694 metabolism in hepatocellular carcinoma. *Metabolites* 9: 36, 2019.
695 29. **Machado BE, and Podrabsky JE**. Salinity tolerance in diapausing embryos of
696 the annual killifish *Austrofundulus limnaeus* is supported by exceptionally low water and

697 ion permeability. *Journal of Comparative Physiology B: Biochemical, Systemic, and*
698 *Environmental Physiology* 177: 809-820, 2007.
699 30.   **Masella R, Di Benedetto R, Varì R, Filesi C, and Giovannini C**. Novel
700 mechanisms of natural antioxidant compounds in biological systems: involvement of
701 glutathione and glutathione-related enzymes. *Journal of Nutritional Biochemistry* 16:
702 577-586, 2005.
703 31.   **Meller CL, Meller R, Simon RP, Culpepper KM, and Podrabsky JE**. Cell cycle
704 arrest associated with anoxia-induced quiescence, anoxic preconditioning, and
705 embryonic diapause in embryos of the annual killifish *Austrofundulus limnaeus*. *Journal*
706 *of Comparative Physiology B* 182: 909-920, 2012.
707 32.   **Mellor D, and Slater J**. Daily changes in amniotic and allantoic fluid during the
708 last three months of pregnancy in conscious, unstressed ewes, with catheters in their
709 foetal fluid sacs. *The Journal of Physiology* 217: 573-604, 1971.
710 33.   **Minard KI, and McAlister-Henn L**. Antioxidant function of cytosolic sources of
711 NADPH in yeast. *Free Radical Biology and Medicine* 31: 832-843, 2001.
712 34.   **Mouchiroud L, Houtkooper RH, Moullan N, Katsyuba E, Ryu D, Cantó C,**
713 **Mottis A, Jo Y-S, Viswanathan M, and Schoonjans K**. The NAD+/sirtuin pathway
714 modulates longevity through activation of mitochondrial UPR and FOXO signaling. *Cell*
715 154: 430-441, 2013.
716 35.   **Nada SE, Tulsulkar J, Raghavan A, Hensley K, and Shah ZA**. A derivative of
717 the CRMP2 binding compound lanthionine ketimine provides neuroprotection in a
718 mouse model of cerebral ischemia. *Neurochemistry international* 61: 1357-1363, 2012.
719 36.   **Nilsson GE, Lutz PL, and Jackson TL**. Neurotransmitters and anoxic survival
720 of the brain: A comparison of anoxia-tolerant and anoxia-intolerant vertebrates.
721 *Physiological Zoology* 64: 638-652, 1991.
722 37.   **Oldham WM, Clish CB, Yang Y, and Loscalzo J**. Hypoxia-mediated increases
723 in L-2-hydroxyglutarate coordinate the metabolic response to reductive stress. *Cell*
724 *metabolism* 22: 291-303, 2015.
725 38.   **Olson KR**. H_2S and polysulfide metabolism: conventional and unconventional
726 pathways. *Biochemical Pharmacology* 149: 77-90, 2018.
727 39.   **Orlowski M, and Meister A**. The γ-glutamyl cycle: a possible transport system
728 for amino acids. *Proceedings of the National Academy of Sciences of the United States*
729 *of America* 67: 1248-1255, 1970.
730 40.   **Pallister T, Jackson MA, Martin TC, Zierer J, Jennings A, Mohney RP,**
731 **MacGregor A, Steves CJ, Cassidy A, and Spector TD**. Hippurate as a metabolomic
732 marker of gut microbiome diversity: modulation by diet and relationship to metabolic
733 syndrome. *Scientific reports* 7: 1-9, 2017.
734 41.   **Patra KC, and Hay N**. The pentose phosphate pathway and cancer. *Trends in*
735 *Biochemical Sciences* 39: 347-354, 2014.
736 42.   **Perna AF, Anishchenko E, Vigorito C, Zacchia M, Trepiccione F, D'Aniello**
737 **S, and Ingrosso D**. Zebrafish, a novel model system to study uremic toxins: the case
738 for the sulfur amino acid lanthionine. *International journal of molecular sciences* 19:
739 1323, 2018.
740 43.   **Podrabsky J, Riggs C, Romney A, Woll S, Wagner J, Culpepper K, and**
741 **Cleaver T**. Embryonic development of the annual killifish *Austrofundulus limnaeus*: An

742 emerging model for ecological and evolutionary developmental biology research and
743 instruction. *Developmental Dynamics* 246: 779-801, 2017.
744 44. **Podrabsky J, Riggs C, and Wagner J**. Tolerance of Environmental Stress. In:
745 *Annual Fishes Life History Strategy, Diversity, and Evolution*, edited by Berois N, García
746 G, and De Sá R. Boca Raton, FL USA: CRC Press, Taylor & Francis, 2016, p. 159-184.
747 45. **Podrabsky JE**. Husbandry of the annual killifish *Austrofundulus limnaeus* with
748 special emphasis on the collection and rearing of embryos. *Environmental Biology of*
749 *Fishes* 54: 421-431, 1999.
750 46. **Podrabsky JE, Carpenter JF, and Hand SC**. Survival of water stress in annual
751 fish embryos: dehydration avoidance and egg envelope amyloid fibers. *American*
752 *Journal of Physiology* 280: R123-R131, 2001.
753 47. **Podrabsky JE, Garrett IDF, and Kohl ZF**. Alternative developmental pathways
754 associated with diapause regulated by temperature and maternal influences in embryos
755 of the annual killifish *Austrofundulus limnaeus*. *Journal of Experimental Biology* 213:
756 3280-3288, 2010.
757 48. **Podrabsky JE, and Hand SC**. The bioenergetics of embryonic diapause in an
758 annual killifish, *Austrofundulus limnaeus*. *Journal of Experimental Biology* 202: 2567-
759 2580, 1999.
760 49. **Podrabsky JE, and Hand SC**. Depression of protein synthesis during diapause
761 in embryos of the annual killifish *Austrofundulus limnaeus*. *Physiological and*
762 *Biochemical Zoology* 73: 799-808, 2000.
763 50. **Podrabsky JE, Hrbek T, and Hand SC**. Physical and chemical characteristics of
764 ephemeral pond habitats in the Maracaibo basin and Llanos region of Venezuela.
765 *Hydrobiologia* 362: 67-78, 1998.
766 51. **Podrabsky JE, Lopez JP, Fan TWM, Higashi R, and Somero GN**. Extreme
767 anoxia tolerance in embryos of the annual killifish *Austrofundulus limnaeus*: Insights
768 from a metabolomics analysis. *Journal of Experimental Biology* 210: 2253-2266, 2007.
769 52. **Polačik M, and Podrabsky JE**. Temporary Environments. In: *Extremophile*
770 *Fishes: Ecology, Evolution, and Physiology of Teleosts in Extreme Environments*, edited
771 by Riesch R, Tobler M, and Plath M. Cham, Switzerland: Springer, 2015, p. 217-245.
772 53. **Polačik M, Vrtílek M, Reichard M, Blazek R, and Podrabsky J**. Embryo
773 ecology: A critical role of environment in the diapause of wild annual fish populations.
774 *Freshwater Biology* submitted: 2020.
775 54. **Romney A, Davis E, Corona M, Wagner J, and Podrabsky J**. Temperature
776 dependent vitamin D signaling regulates developmental trajectory associated with
777 diapause in an annual killifish. *Proceedings of the National Academy of Sciences of the*
778 *United States of America* 115: 12763-12768, 2018.
779 55. **Rust C, Karnitz LM, Paya CV, Moscat J, Simari RD, and Gores GJ**. The bile
780 acid taurochenodeoxycholate activates a phosphatidylinositol 3-kinase-dependent
781 survival signaling cascade. *Journal of Biological Chemistry* 275: 20210-20216, 2000.
782 56. **Saks V, and Strumia E**. Phosphocreatine: molecular and cellular aspects of the
783 mechanism of cardioprotective action. *Current Therapeutic Research* 53: 565-598,
784 1993.
785 57. **Schoots AFM, Stikkelbroeck JJM, Bekhuis JF, and Denuce JM**. Hatching in
786 teleostean fishes: fine structural changes in the egg envelope during enzymatic
787 breakdown *in vivo* and *in vitro*. *Journal of Ultrastructure Research* 80: 185-196, 1982.

788   58.   **Spustova V, and Oravec C**. Antitumor effect of hippurate. An experimental
789   study using various mouse tumor strains. *Neoplasma* 36: 317-320, 1989.
790   59.   **Steele SL, Chadwick TD, and Wright PA**. Ammonia detoxification and
791   localization of urea cycle enzyme activity in embryos of the rainbow trout
792   (*Oncorhynchus mykiss*) in relation to early tolerance to high environmental ammonia
793   levels. *Journal of Experimental Biology* 204: 2145-2154, 2001.
794   60.   **Tarasenko TN, Cusmano-Ozog K, and McGuire PJ**. Tissue acylcarnitine status
795   in a mouse model of mitochondrial β-oxidation deficiency during metabolic
796   decompensation due to influenza virus infection. *Molecular Genetics and Metabolism*
797   125: 144-152, 2018.
798   61.   **Tauffenberger A, Fiumelli H, Almustafa S, and Magistretti PJ**. Lactate and
799   pyruvate promote oxidative stress resistance through hormetic ROS signaling. *Cell*
800   *Death & Disease* 10: 1-16, 2019.
801   62.   **Tokarska-Schlattner M, Epand RF, Meiler F, Zandomeneghi G, Neumann D,**
802   **Widmer HR, Meier BH, Epand RM, Saks V, and Wallimann T**. Phosphocreatine
803   interacts with phospholipids, affects membrane properties and exerts membrane-
804   protective effects. *PLoS One* 7: 2012.
805   63.   **Vigorito C, Anishchenko E, Mele L, Capolongo G, Trepiccione F, Zacchia M,**
806   **Lombari P, Capasso R, Ingrosso D, and Perna AF**. Uremic toxin lanthionine
807   interferes with the transsulfuration pathway, angiogenetic signaling and increases
808   intracellular calcium. *International journal of molecular sciences* 20: 2269, 2019.
809   64.   **Wagner J, Singh P, Romney A, Riggs C, Minx P, Woll S, Roush J, Warren**
810   **W, Brunet A, and Podrabsky J**. The genome of *Austrofundulus limnaeus* offers
811   insights into extreme vertebrate stress tolerance and embryonic development. *BMC*
812   *Genomics* 19: 155, 2018.
813   65.   **Wagner JT, Knapp MJ, and Podrabsky JE**. Antioxidant capacity and anoxia
814   tolerance in *Austrofundulus limnaeus* embryos. *Journal of Experimental Biology* 222:
815   jeb204347, 2019.
816   66.   **Ward PS, Patel J, Wise DR, Abdel-Wahab O, Bennett BD, Coller HA, Cross**
817   **JR, Fantin VR, Hedvat CV, and Perl AE**. The common feature of leukemia-associated
818   IDH1 and IDH2 mutations is a neomorphic enzyme activity converting α-ketoglutarate to
819   2-hydroxyglutarate. *Cancer Cell* 17: 225-234, 2010.
820   67.   **Williams M, Wallace S, Tyler J, McCall C, Gutierrez A, and Spano J**.
821   Biochemical characteristics of amniotic and allantoic fluid in late gestational mares.
822   *Theriogenology* 40: 1251-1257, 1993.
823   68.   **Winston PW, and Bates DH**. Saturated solutions for the control of humidity in
824   biological research. *Ecology* 41: 232-237, 1960.
825   69.   **Wourms JP**. The developmental biology of annual fish II. Naturally occuring
826   dispersion and reaggregation of blastomeres during the development of annual fish
827   eggs. *Journal of Experimental Zoology* 182: 169-200, 1972.
828   70.   **Wourms JP**. The developmental biology of annual fishes I. Stages in the normal
829   development of *Austrofundulus myersi* Dahl. *Journal of Experimental Zoology* 182: 143-
830   168, 1972.
831   71.   **Wourms JP**. The developmental biology of annual fishes III. Pre-embryonic and
832   embryonic diapause of variable duration in the eggs of annual fishes. *Journal of*
833   *Experimental Zoology* 182: 389-414, 1972.

834 72.   **Wright PA, Felskie A, and Anderson PM**. Induction of ornithine-urea cycle
835 enzymes and nitrogen metabolism and excretion in rainbow trout (*Oncorhynchus*
836 *mykiss*) during early life stages. *Journal of Experimental Biology* 198: 127-135, 1995.
837 73.   **Xu W, Yang H, Liu Y, Yang Y, Wang P, Kim S-H, Ito S, Yang C, Wang P, and**
838 **Xiao M-T**. Oncometabolite 2-hydroxyglutarate is a competitive inhibitor of α-
839 ketoglutarate-dependent dioxygenases. *Cancer Cell* 19: 17-30, 2011.
840 74.   **Zajic D, Nicholson J, and Podrabsky J**. No water, no problem: Stage-specific
841 metabolic responses to dehydration stress in annual killifish embryos. *Journal of*
842 *Experimental Biology* Accepted: 2020.
843 75.   **Zajic D, and Podrabsky J**. GABA daba doo, anoxia got nothing on you: GABA
844 metabolism is crucial for long-term survival in annual killifish embryos. *Journal of*
845 *Experimental Biology* Submitted: 2020.
846 76.   **Zazueta C, Buelna-Chontal M, Macías-López A, Román-Anguiano NG,**
847 **González-Pacheco H, Pavón N, Springall R, Aranda-Frausto A, Bojalil R, and**
848 **Silva-Palacios A**. Cytidine-5'-diphosphocholine protects the liver from
849 ischemia/reperfusion injury preserving mitochondrial function and reducing oxidative
850 stress. *Liver Transplantation* 24: 1070-1083, 2018.
851 77.   **Zhang D, Tang Z, Huang H, Zhou G, Cui C, Weng Y, Liu W, Kim S, Lee S,**
852 **and Perez-Neut M**. Metabolic regulation of gene expression by histone lactylation.
853 *Nature* 574: 575-580, 2019.
854 78.   **Zweifler RM**. Membrane stabilizer: citicoline. *Current Medical Research and*
855 *Opinion* 18: s14-s17, 2002.
856

Figure Captions

859 **Figure 1. Schematic of the experimental design and sampling regimen used for**

860 **metabolomics analysis.** Embryos were exposed to 85% relative humidity (RH) at the

861 developmental stage listed (DII or WS 36) for up to 28 d ($N = 6$, each replicate

862 contained 25 embryos). Developmental stage at time of sampling is included below

863 each timepoint. WS, Wourms' stage; DII, diapause II.

864

865 **Figure 2. Heat maps of fold change from t = 0 of 673 metabolites detected in**

866 **embryos.**

867 Heat maps (organized by superpathway) represent the $\log_2$ fold change of each

868 metabolite in response to short-term (S) and long-term (L) aerial dehydration stress in

869 diapause II (DII) and post-DII embryos when compared to control embryos at t = 0.

870 Metabolites are clustered by subpathways. Major subpathways are indicated on the left

871 of each heat map. Within each heatmap, fold changes are displayed for all

872 comparisons, even though fold changes may not be statistically significant for all

873 columns. For details on sampling, see Figure 1.

874

875 **Figure 3. Shared metabolites that significantly change during long-term aerial**

876 **dehydration stress in DII and post-DII embryos.** A total of 18 metabolites decreased

877 and 71 metabolites increased in both stages. Values are $\log_2$ fold changes relative to t =

878 0. The vertical dotted line separates the downregulated (left) and upregulated (right)

879 metabolites. The color of each metabolite denotes superpathway. Metabolites with

880 asterisks indicate compounds that have not been confirmed based on standards, but

881 Metabolon is confident in their identity.

882

883 **Figure 4. Indications of altered transsulfuration activity and antioxidant utilization**

884 **in DII and post-DII embryos.** Box plot data illustrating metabolites contributing to

885 methionine, cysteine, and glutathione metabolism. Data (scaled intensity) are presented

886 as box plots with a line drawn at the median (mean indicated by a plus symbol) and the

887 box indicating upper and lower quartiles. Error bars are distribution minimums and

888 maximums. Vertical dotted lines separate data from DII (blue) and post-DII embryos

889 (orange). Data are organized by aerial exposure treatment (C, control; S, short-term; L,

890 long-term). Asterisks represent metabolites that were significantly different from t = 0

891 (Welch's two-sample t-test, $P < 0.05$). Raw values for each metabolite were scaled to

892 set the median across all samples to 1 and were normalized to DNA content. Relevant

893 enzymes are included (grey boxes). CBS, cystathionine β-synthase; CSE, cystathionine

894 γ-lyase; GCS, gamma-glutamylcysteine synthetase; GS, glutathione synthase; GGT,

895 gamma-glutamyl transferase.

896

897 **Figure 5. Changes in gamma-glutamyl amino acid metabolism in DII and post-DII**

898 **embryos.** Box plots illustrating metabolites involved in gamma-glutamyl amino acid

899 metabolism that were significantly altered in at least one stage. For details of box plots

900 and presentation of scaled intensity data, please see the legend of Figure 4. Asterisks

901 represent metabolites that were significantly different from t = 0 (Welch's two-sample t-

902 test, $P < 0.05$). Gamma-glutamylisoleucine (asterisk) had not been confirmed based on

903 a standard, but Metabolon is confident in the identity.

904

905 **Figure 6. Changes in creatine metabolism in DII and post-DII embryos.** Box plots

906 illustrating metabolites involved in creatine metabolism. For details of box plots and

907 presentation of scaled intensity data, please see the legend of Figure 4. Asterisks

908 represent metabolites that were significantly different from t = 0 (Welch's two-sample t-

909 test, $P < 0.05$).

910

911 **Figure 7. Changes in glycolysis and pentose phosphate pathway metabolism in**

912 **DII and post-DII embryos.** Box plots illustrating metabolites involved in glycolysis and

913 pentose phosphate pathway (PPP) metabolism. For details of box plots and

914 presentation of scaled intensity data, please see the legend of Figure 4. Asterisks

915 represent metabolitrs that were significantly different from t = 0 (Welch's two-sample t-

916 test, $P < 0.05$).

917

918 **Figure 8. Changes in nicotinate and nicotinamide metabolism in DII and post-DII**

919 **embryos.** Box plots illustrating metabolites contributing to nicotinate and nicotinamide

920 metabolism. For details of box plots and presentation of scaled intensity data, please

921 see the legend of Figure 4. Asterisks represent metabolites that were significantly

922 different from t = 0 (Welch's two-sample t-test, $P < 0.05$).

923

Dehydration exposure

	Control	Short-term	Long-term	
DII	t = 0 d (DII)	t = 7 d (DII)	t = 28 d (DII)	Dormant
Post-DII	t = 0 d (WS 36)	t = 7 d (WS 40)	t = 18 d (WS 42/43)	Actively developing

Lipid

Long Chain
Fatty Acid

Polyunsaturated
n3 and n6

Dicarboxylate

Acyl Carnitine

Acyl Choline
Monohydroxy
Dihydroxy

Endocannabinoid

Phospholipid
Metabolism

Phosphatidylcholine
(PC)

Phosphatidylethanolamine
(PE)

Lysophospholipid

Plasmalogen

Monoacylglycerol

Diacylglycerol

Ceramides

Dihydrosphingomyelins

Sphingomyelins

Sterol

Bile metabolism

Amino Acid

Gly, Ser,
and Thr
Ala and Asp
Glu
His
Lys
Phe
Tyr
Trp
Leu, Ile,
and Val
Met, Cys, SAM,
and Taurine
Urea cycle;
Arg and Pro
Creatine
Polyamine
Glutathione

Carbohydrate

Glycolysis,
Gluconeogenesis,
and Pyruvate
Pentose
Glycogen
Fructose, Mannose,
Galactose
Aminosugar

S L S L
DII Post-DII

Peptide

Gamma-glutamyl
Amino Acid

Dipeptide

Energy

TCA Cycle

Cofactors and Vitamins

Nicotinate and
Nicotinamide

Pterin

Vitamin A and B6

Xenobiotics

Food Component/
Plant

Drug - Topical Agents
Chemical

Nucleotide

Purine:
Xanthine/Inosine
Purine: Adenine
Purine: Guanine
Pyrimidine: Orotate
Pyrimidine: Uracil
Pyrimidine: Cytidine
Pyrimidine: Thymine
Dinucleotide

-5 0 5 10
Log$_2$ (fold change)

Stage legend: DII (blue), Post-DII (orange)

Superpathway:
- Xenobiotics (black)
- Cofactors and Vitamins (red)
- Nucleotide (dark blue)
- Lipid (magenta/pink)
- Carbohydrate (light blue)
- Peptide (gray)
- Amino Acid (green)

Right panel metabolites (top to bottom):
- salicylate
- benzoylcarnitine*
- hippurate
- hydroquinone sulfate
- p-cresol sulfate
- guaiacol sulfate
- nicotinamide
- 5-methyl-2'-deoxycytidine
- inosine
- thymidine
- guanosine
- 2'-deoxyinosine
- uridine
- allantoin
- palmitoleoylcarnitine (C16:1)*
- sebacate (C10-DC)
- maleate
- 1-linoleoyl-GPE (18:2)*
- 1-(1-enyl-stearoyl)-GPE (P-18:0)*
- taurolithocholate
- stearoylcarnitine (C18)
- 1-(1-enyl-palmitoyl)-2-oleoyl-GPE (P-16:0/18:1)*
- docosapentaenoylcarnitine (C22:5n6)*
- 1-arachidonoyl-GPE (20:4n6)*
- 3-methylglutarate/2-methylglutarate
- arachidonoylcarnitine (C20:4)
- adipate (C6-DC)
- glutarate (C5-DC)
- N-stearoyl-sphingosine (d18:1/18:0)*
- ceramide (d18:1/17:0, d17:1/18:0)*
- 1-(1-enyl-palmitoyl)-2-arachidonoyl-GPE (P-16:0/20:4)*
- ceramide (d18:2/24:1, d18:1/24:2)*
- arachidoylcarnitine (C20)*
- cytidine-5'-diphosphoethanolamine
- 3-hydroxyadipate*
- 2-hydroxyglutarate
- cytidine 5'-diphosphocholine
- taurochenodeoxycholate
- arabonate/xylonate
- arabitol/xylitol
- pyruvate
- N-acetyl-glucosamine 1-phosphate
- glucuronate
- glucose 6-phosphate
- lactate
- sedoheptulose-7-phosphate
- gamma-glutamyltryptophan
- N-acetylarginine
- N,N,N-trimethyl-alanylproline betaine (TMAP)
- phenylpyruvate
- 4-hydroxyphenylpyruvate
- methylsuccinate
- 1-methyl-5-imidazoleacetate
- C-glycosyltryptophan
- 4-methyl-2-oxopentanoate
- N-acetyltaurine
- N-acetylhistidine
- cyano-alanine
- N-acetyl-isoputreanine*
- 2,3-dihydroxy-5-methylthio-4-pentenoate (DMTPA)*
- 1-methyl-4-imidazoleacetate
- 3-methoxytyrosine
- argininate*
- gamma-aminobutyrate (GABA)
- cystathionine
- picolinate
- glutathione, oxidized (GSSG)
- N2-acetyllysine
- phenol sulfate
- N-acetyl-1-methylhistidine*
- lanthionine

Left panel metabolites (bottom section, top to bottom):
- pheophytin A
- nicotinamide ribonucleotide (NMN)
- nicotinate
- N-carbamoylaspartate
- adenosine
- 1-oleoylglycerol (18:1)
- 1-docosahexaenoylglycerol (22:6)
- 1-heptadecenoylglycerol (17:1)*
- 1-linoleoylglycerol (18:2)
- 1-myristoylglycerol (14:0)
- 2-heptadecenoylglycerol (17:1)*
- 2-docosahexaenoylglycerol (22:6)*
- 1-dihomo-linolenylglycerol (20:3)
- 1-palmitoleoylglycerol (16:1)*
- 1-arachidonylglycerol (20:4)
- 2-palmitoleoylglycerol (16:1)*
- sucrose
- ophthalmate

X-axis (both panels): Log$_2$ (fold change), left panel range −10 to 0, right panel range 0 to 10

Figure showing box plots of scaled intensity for various gamma-glutamyl amino acid metabolites across DII and Post-DII groups (C, S, L).

Row 1: gamma-glutamyl-2-aminobutyrate; gamma-glutamylalanine; gamma-glutamyl-alpha-lysine; gamma-glutamylglutamate

Row 2: gamma-glutamylglutamine; gamma-glutamylglycine; gamma-glutamylhistidine; gamma-glutamylisoleucine*

Row 3: gamma-glutamylleucine; gamma-glutamylmethionine; gamma-glutamylphenylalanine; gamma-glutamylserine

Row 4: gamma-glutamylthreonine; gamma-glutamyltryptophan; gamma-glutamyltyrosine; gamma-glutamylvaline

Legend: DII (blue), Post-DII (orange)

Y-axis: Scaled intensity

X-axis categories: C, S, L

Arginine

Glycine

Ornithine

Guanidinoacetate

ADP → ATP

Creatine phosphate ⇌ Creatine

ATP → ADP

Creatinine

Legend:
- DII (blue)
- Post-DII (orange)

Glycolysis

glucose

↓

glucose 6-phosphate

→ **Pentose Phosphate Pathway**

NADP+
NADPH

↓

fructose 6-phosphate

↓

fructose 1,6-biphosphate

↓

glyceraldehyde 3-phosphate

↓

1,3-biphosphoglycerate

↓

3-phosphoglycerate → **glycerate**

↓

2-phosphoglycerate

↓

phosphoenolpyruvate (PEP)

↓

pyruvate → **lactate**

Pentose Phosphate Pathway:
ribulose 5-phosphate

xylulose 5-phosphate   ribose 5-phosphate

glyceraldehyde 3-phosphate   **sedoheptulose 7-phosphate**

↓

fructose 6-phosphate
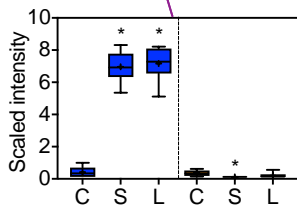
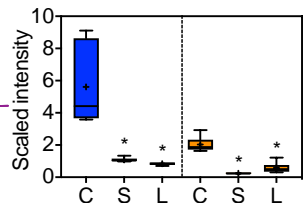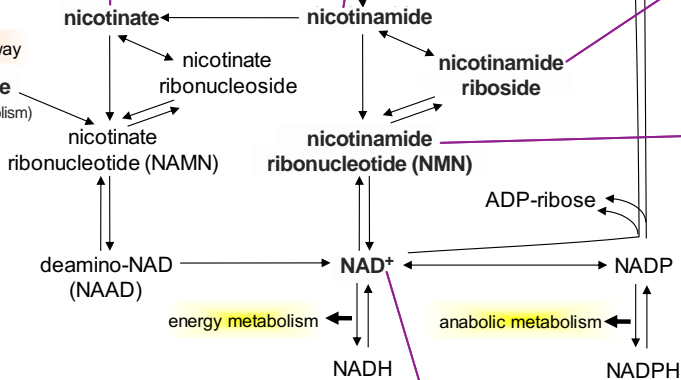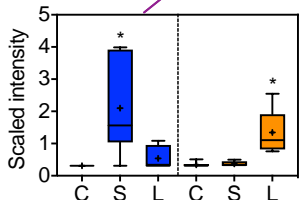Axis labels for box plots: Scaled intensity; categories C, S, L

Table 1. Total number of significant metabolites (among 673 total metabolites identified) that were significantly affected by short and long-term aerial dehydration stress in DII and post-DII embryos initially exposed at WS 36.

Stage	Comparison	Non-normalized		Protein-normalized		DNA-normalized	
		Total metabolites $P < 0.05$	Metabolites (up | down)	Total metabolites $P < 0.05$	Metabolites (up | down)	Total metabolites $P < 0.05$	Metabolites (up | down)
DII	7 d / 0 d (short-term)	243	156 | 87	238	85 | 153	204	174 | 30
	28 d / 0 d (long-term)	346	298 | 48	200	77 | 123	267	233 | 34
Post-DII	7 d / 0 d (short-term)	466	383 | 83	438	269 | 169	553	74 | 479
	18 d / 0 d (long-term)	558	430 | 128	544	354 | 190	390	212 | 178

Table 2. Metabolic pathways that were significantly enriched by short and long-term aerial dehydration stress in DII and post-DII embryos normalized to DNA concentration.

Treatment (# significant metabolites)	Subpathway	Enrichment Value	P-value	k	m
DII short-term (n = 204)	Fatty Acid, Dihydroxy	3.3	0.03	3	3
	Fatty Acid, Dicarboxylate	2.6	6.34E-04	10	13
	Fatty Acid, Monohydroxy	2.4	0.03	5	7
	Nicotinate and Nicotinamide Metabolism	2.4	0.03	5	7
	Tyrosine Metabolism	2.4	0.01	7	10
	Methionine, Cysteine, SAM and Taurine Metabolism	2.0	4.17E-03	13	22
	Leucine, Isoleucine and Valine Metabolism	1.9	0.02	11	20
DII long-term (n = 267)	Fatty Acid Metabolism (Acyl Carnitine, Long Chain Saturated)	1.9	0.05	6	8
	Tyrosine Metabolism	1.8	0.05	7	10
	Monoacylglycerol	1.7	0.03	11	17
	Methionine, Cysteine, SAM and Taurine Metabolism	1.6	0.02	14	22
Post-DII short-term (n = 553)	Phosphatidylcholine (PC)	1.2	0.02	19	19
	Urea cycle; Arginine and Proline Metabolism	1.2	0.02	19	19
	Gamma-glutamyl Amino Acid	1.2	0.03	17	17
	Monoacylglycerol	1.2	0.03	17	17
	Diacylglycerol	1.2	7.71E-03	34	35
Post-DII long-term (n = 390)	Aminosugar Metabolism	1.7	0.01	8	8
	Purine Metabolism, Adenine containing	1.6	0.03	9	10
	Gamma-glutamyl Amino Acid	1.5	7.36E-03	15	17
	Monoacylglycerol	1.5	7.36E-03	15	17
	Phosphatidylcholine (PC)	1.5	0.01	16	19

Enrichment value was computed as follows: (k/m)/((n-k)/(N-m)), where: k, total number of significant metabolites in pathway; m, total number of detected metabolites in pathway; n, total number of significant metabolites; N, total number of detected metabolites (673). A pathway enrichment value greater than one indicates that the pathway contained more significantly changed metabolites relative to the study overall. Fisher's exact test was used to determine if pathway enrichment was significant (P < 0.05).